

An Experimental and Numerical Study of Q -Switched Mode-Locking in Monolithic Semiconductor Diode Lasers

Michael B. Flynn, *Student Member, IEEE*, Liam O'Faolain, and Thomas F. Krauss

Abstract—We present experimental results of Q -switched mode-locking (QML) of a monolithic two-section semiconductor laser. We demonstrate tuning of the Q -switched envelope repetition rate with pumping current over the range of 0.4 to 1.6 GHz. Detailed numerical modeling is used to study a range of similar devices and to investigate the mechanisms and conditions for QML to occur. We also discuss design conditions for increasing the tuning up to 4 GHz.

Index Terms—Mode-locked lasers, modeling, pulsed lasers, Q -switched lasers, semiconductor lasers.

I. INTRODUCTION

SEMICONDUCTOR lasers offer many attractive features for ultrashort pulse generation. They are low cost, electrically pumped and their output can easily be coupled into fibers. In particular, by placing all of the elements for pulse generation on a single chip of about 1 mm in length one can achieve extreme compactness and avoid mechanical instabilities associated with external cavities.

In this work we consider a two-section amplifier/absorber monolithic diode laser [1] (see Fig. 1). The longer amplifier section is forward biased to provide gain and the shorter section is reverse biased to form a slow saturable absorber. We examine the operating behavior of such a device with a particular emphasis on the Q -switched modelocking (QML) regime [2]. This regime consists of a longer Q -switched envelope with an underlying train of mode-locked pulses. The Q -switched envelope has a repetition rate of the order of 1 GHz allowing the 40-GHz mode-locked pulses to have much higher peak powers than for a continuous-wave (CW) mode-locked similar device.

We can tune the output frequency of the device by varying the current to the gain section. Higher currents lead to higher frequencies. However, we can only encounter QML within a specific range of currents for any given device, if at all. This is because QML is conditional on a sensitive balance between gain and loss which may not be possible within certain device configurations.

We constructed a device that allowed a frequency tuning over a range of 0.4–1.6 GHz. Frequency tuning of self-pulsating (SP) diode lasers has been studied in [3] which showed tuning of 1 to 4 GHz. However, despite similarities with QML, self-pulsation

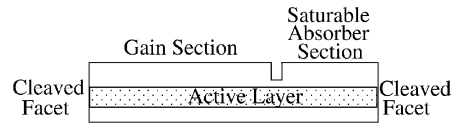


Fig. 1. Diagram of two-section monolithic diode laser structure.

is passive Q -switching with a noisy filling within the envelope instead of a train of mode-locked pulses.

Passively mode-locked (PML) two-section diode lasers have been made in lengths from 7 to 0.25 mm corresponding to the frequencies of 5.5 [4] to 350 GHz [5]. QML allows us to extend the repetition rate of our devices from this lower PML frequency down into the megahertz range, while also keeping the ultrashort mode-locked pulses within our signal under the envelope.

Although many applications of ultrashort pulses such as telecommunications require stable mode-locking with steady pulse energy, there are a number of applications where increased peak powers are extremely advantageous. An example is that of nonlinear frequency conversion. Generation of blue light is of particular interest for medical diagnostics and optical data storage. As Q -switched mode-locked pulses can have peak powers many times higher than that of mode-locked pulses for similar current injection, much better second harmonic generation could be obtained.

Another possible area of application is that of precise fabrication of microstructures [6]. For pulses of the order of 1 ps and shorter, the average ablation rate is dependent on the optical penetration depth for low laser fluences. For longer pulses, only the effective heat penetration depth which is independent of pulse duration is an issue. QML would allow the use of picosecond pulses but with much higher peak powers than simply mode-locked pulses. As power output from diode lasers increase this may prove to be a very practical, compact and suitable source for micromachining.

The use of ultrashort pulses in surgery has been examined in [7]. Primarily Q -switched CO₂ and Nd:YAG lasers are used, however heat diffusion typically leads to adjacent tissue being damaged. The use of short pulses leads to plasma-mediated ablation which does not exhibit damaging thermal effects and also yields much better precision. It has also been found that the ablation efficiency for shorter pulses is greater than that for longer pulses with the same pulse energy. The use of mode-locked pulses would seem an obvious choice for such an application and by putting a Q -switched envelope over these pulses it also gives us freedom to control the repetition rate. This offers a distinct advantage in that one would have greater control over the

Manuscript received December 22, 2003; revised April 23, 2004.

The authors are with the Ultrafast Photonics Collaboration, School of Physics and Astronomy, University of St. Andrews, North Haugh, Fife KY16 9SS, U.K. (e-mail: mbf@st-and.ac.uk).

Digital Object Identifier 10.1109/JQE.2004.831623

TABLE I
WAVEGUIDE LAYER PARAMETERS

Layer Name	Material	Thickness
Cap	p+ GaAs	0.1 μm
Top Clad	AlGaAs (p=8e17cm ⁻³)	0.3 μm
Barrier	GaAs	0.12 μm
QW	In _{0.18} Ga _{0.78} As	75 \AA
Barrier	GaAs	100 \AA
QW	In _{0.18} Ga _{0.78} As	75 \AA
Barrier	GaAs	0.12 μm
Bottom Clad	AlGaAs (n=8e17cm ⁻³)	1 μm
Substrate	n+ GaAs	

ablation rate. There is also an efficiency argument to be made for QML over a mode-locked source in that for the same electrical input QML delivers peak powers several times greater.

A final example of an application of QML is that of the measurement of two-photon absorption (TPA) by loss modulation [8] which can often be difficult due to a weak TPA signal. If an intensity modulated ultrashort pulse train is passed through a sample, sidebands will be generated on the main mode-locking frequency which can then be measured very accurately. This technique has the advantage that it does not rely on fluorescent constraints and could be adapted for measuring higher-order nonlinear absorption also.

These applications have been previously studied in the literature with respect to bulky solid-state laser sources. QML in semiconductor lasers has not received much attention in the literature largely due to its unsuitability for communication applications. However, as output power from diode lasers improves, QML may prove to be a very valuable and practical method for producing high energy ultrashort pulses with controllable repetition rate from an electrically pumped, highly compact and cheap source.

In this paper we show experimental results of QML in a monolithic two-section semiconductor diode laser. We obtain a QML frequency tuning relationship with driving current. In addition, we provide numerical simulations which display the same behavior and allow us to extrapolate to other devices. We also describe the onset of QML and discuss the transition to this behavior from other regimes. We produce and discuss our experimental results in Section II. Section III introduces our model and device parameters. Section IV deals with our numerical simulations and results. Finally, we present our conclusions.

II. EXPERIMENTAL RESULTS

We fabricated a simple two-section laser comprised of a 1080- μm -long gain section and a 200- μm -long saturable absorber section. The two sections were isolated using a 25- μm -wide, 200-nm-deep trench. This had an electrical resistance of approximately 1 k Ω . The GaAs active layer had thin (400 nm) p-type cladding and contained two InGaAs quantum wells. The material was grown by metal-organic vapor phase epitaxy (MOVPE). The wafer details are given in Table I. The output was examined using a 25-GHz RF spectrum analyzer and fast photodiode. Experimentally, no pulsing is detected when the absorber was open circuit. The threshold current of the device was approximately 40 mA. There was insufficient power to take measurements for currents below 50 mA. With

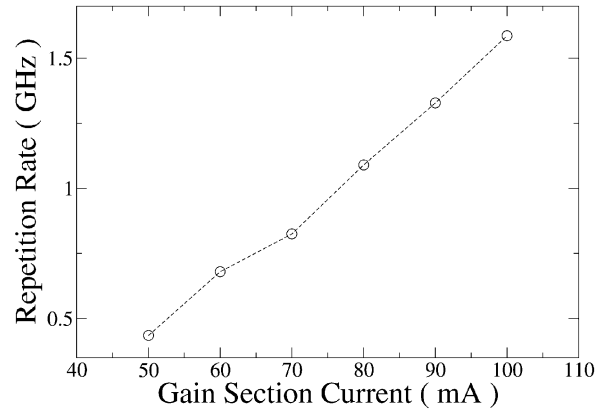


Fig. 2. Measured current-frequency tuning curve for two-section monolithic diode laser.

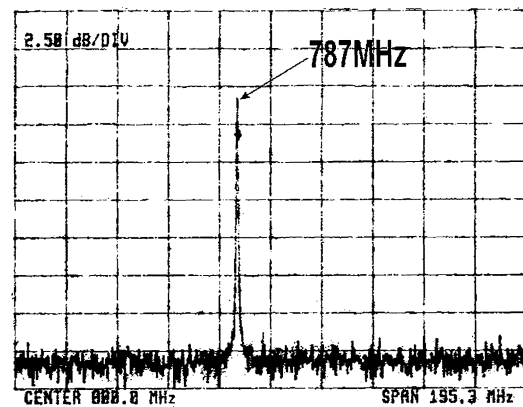


Fig. 3. RF spectra of QML frequency of 787.8 MHz.

the absorber grounded, the device showed pulsing in the range 400 MHz to 1.6 GHz, depending on the applied current. A corresponding abrupt change in the optical spectrum width from 0.5 nm to over 3 nm was observed, indicating mode-locking. A tuning curve is displayed in Fig. 2. A sample RF spectrum is displayed in Fig. 3. All RF spectra were found to be stable.

QML characteristics were observed when the device was in a range of currents just above threshold. In the case of higher or lower currents, no RF spectrum trace could be detected, suggesting behavior had changed to PML. A number of other devices with similar gain length but shorter absorber lengths were fabricated and no pulsing at megahertz frequency was detected.

III. THEORETICAL MODEL

We model our device based on an adapted and extended from of that reported in [9]. The electric field E in the laser diode waveguide can be decomposed into a forward (E^+) and a backward (E^-) travelling wave with

$$E(z, t) = [E^+(z, t)e^{-i\beta_0 z} + E^-(z, t)e^{i\beta_0 z}]e^{-i\omega_0 t} \quad (1)$$

where ω_0 is the reference frequency and β_0 is the propagation constant. These complex forward and backward travelling slowly varying complex envelopes satisfy the equation

$$\left(\frac{\partial}{\partial t} \pm v_g \frac{\partial}{\partial z}\right) E^\pm(z, t) = \frac{(\nu_g \Gamma g - \kappa)}{2} E^\pm(z, t). \quad (2)$$

The group velocity is denoted by ν_g , Γ is the confinement factor, κ is the internal absorption. The photon density is calculated from

$$S(z, t) = |E^+(z, t)|^2 + |E^-(z, t)|^2. \quad (3)$$

We model the complex nonlinear gain g using [10]

$$g_0(z, t) = g_n \frac{(N(z, t) - N_0)(1 + i\alpha)}{1 + \epsilon S(z, t)} \quad (4)$$

$$\frac{\partial g(z, t)}{\partial t} = \frac{g_0(z, t) - g(z, t)}{t_{nl}}. \quad (5)$$

We use g_n for the differential gain with respect to carrier density. N_0 is the carrier density at transparency, α is the linewidth enhancement factor, ϵ is the gain compression factor, and t_{nl} is the gain nonlinearity relaxation time. Gain/absorber saturation is included through the $1 + \epsilon S$ term. Self-phase modulation results in a change in the refractive index of the material due to the linewidth enhancement factor and is realized in the $i\alpha$ term. The finite gain relaxation is accounted for in (5).

The dynamics of the carrier concentration N are modeled with the following rate equation:

$$\frac{\partial N(z, t)}{\partial t} = \frac{J}{ed} - \frac{N}{\tau_n} + BN^2 + CN^3 - \nu_g \Re(g) S. \quad (6)$$

The current density is denoted by J (set to zero in the absorber section), d is the active region thickness, τ_n , is the carrier lifetime and separate values are assigned for the gain and absorber sections, and B and C are the bimolecular and Auger recombination rates, respectively. We note that in the saturable absorber section $N < N_0$ generally, and from (4), we see that we experience a loss (i.e., $|g| < 0$).

The model is easily adaptable to colliding pulse mode-locking or self-colliding pulse mode-locking [10]–[12] through the addition of an extra term to represent coupling between the forward and backward travelling waves in the absorber section.

Spontaneous emission was modeled by adding a nonzero complex Gaussian excitation term to the travelling wave equations [13]. This is necessary to ensure self-starting and to represent noise within the laser cavity.

To account for the finite spectral gain bandwidth of the device a first order infinite impulse response (IIR) filter was implemented similar to that described in [14] and [15]. We use a filter with a frequency response given by

$$|H(\omega)|^2 = \frac{(1 - a)^2}{1 + a^2 - 2a \cos((\omega - \omega_p)\Delta t)}. \quad (7)$$

The filter is implemented using

$$y_{t+\Delta t} = Ay_t + (1 - A)x_t \quad (8)$$

where y_t and x_t are, respectively, the output and input of the digital filter at time t . The magnitude of the complex number A is less than unity and determines the bandwidth of the filter around the peak frequency ω_p through

$$A = a \exp(i\omega_p \Delta t). \quad (9)$$

TABLE II
TYPICAL PARAMETER VALUES USED IN THE SIMULATIONS

Symbol	Description	Value
ν_g	Group velocity of light	0.857×10^{10} cm/s
Γ	Confinement factor	0.02
κ	Internal dissipative loss	2.5 cm^{-1}
N_0	Carrier density at transparency	$1.2 \times 10^{18} \text{ cm}^{-3}$
$g_{n,g}$	Differential gain at transparency (gain)	$1.06 \times 10^{-15} \text{ cm}^2$
$g_{n,a}$	Differential gain at transparency (abs.)	$3.0 \times 10^{-15} \text{ cm}^2$
ϵ_g	Gain compression factor (gain)	$3.0 \times 10^{-17} \text{ cm}^3$
ϵ_a	Gain compression factor (abs.)	$7.7 \times 10^{-17} \text{ cm}^3$
α_g	Linewidth enhancement factor (gain)	3.2
α_a	Linewidth enhancement factor (abs.)	1.24
d	Active layer thickness	$0.01 \text{ }\mu\text{m}$
τ_g	Nonradiative recombination rate (gain)	10 ns
R_1	Reflection at gain facet	0.3
R_2	Reflection at absorber facet	0.3
L_g	Length of gain section	$1000 \text{ }\mu\text{m}$
L_a	Length of absorber section	$200 \text{ }\mu\text{m}$
Δz	Length of spatial integration step	$2 \text{ }\mu\text{m}$
B	Bimolecular recombination constant	$2.5 \times 10^{-10} \text{ cm}^3/\text{s}$
C	Auger recombination rate	$5 \times 10^{-29} \text{ cm}^6/\text{s}$
ω_p	Peak frequency	$3.28676 \times 10^{14}/\text{s}$
a	IIR filter parameter	0.003

We pick A by fitting the frequency response to a standard gain curve for the diode material.

Equation (2) was solved subject to the standard reflection boundary conditions applied at the facets of the laser

$$E^+(z = 0, t) = \sqrt{R_1} E^-(z = 0, t) \quad (10)$$

$$E^-(z = L, t) = \sqrt{R_2} E^+(z = L, t). \quad (11)$$

We approximate the spatial and temporal derivatives in the two advection equations (2) by first-order difference approximations. By neglecting the second derivatives, we can use the following approximation [16]:

$$E^\pm(z \pm \Delta z, t + \Delta t) - E^\pm(z, t) \approx \frac{\partial E^\pm}{\partial t} \Delta t \pm \frac{\partial E^\pm}{\partial z} \Delta z \quad (12)$$

where Δz is the spatial integration step and $\Delta t = \Delta z/\nu_g$.

The parameter values used for the simulations were selected based on a standard InGaAs QW based device. Table II gives an explanation of parameters and their values.

IV. NUMERICAL RESULTS

A. Transition From CW Mode-Locking to QML

As discussed in [14], there are four distinct types of pulsed output from two-section monolithic diode lasers. These types are CW mode-locking, unstable mode-locking, QML, and self-pulsation. The type of pulsed output depends on many parameters but normally for a given device we can switch from one type of behavior to another by changing the pumping current and/or the reverse bias on the saturable absorber. We show the transition from CW mode-locking to QML through the intermediate unstable mode-locking in Fig. 4.

CW mode-locking yields trains of mode-locked pulses with good amplitude stability. Unstable mode-locking also gives trains of mode-locked pulses at the round-trip of the laser cavity, however the amplitude of the pulses tends to vary and the mode-locking is not as stable. QML sees the mode-locked

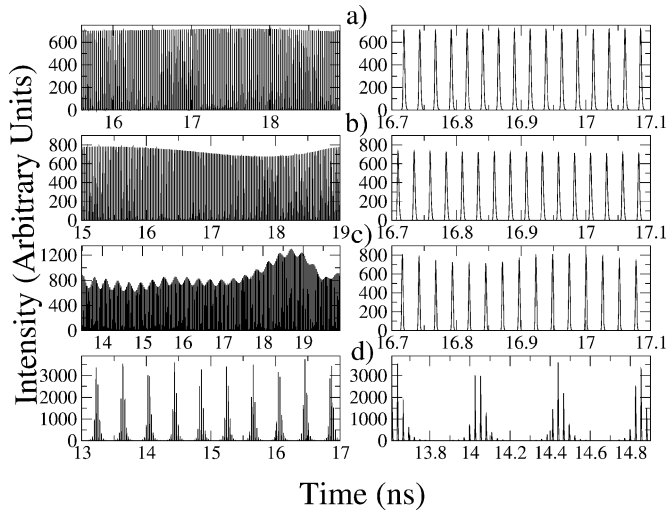


Fig. 4. Transition from CW mode-locking to QML for monolithic diode laser for $\tau_a = 35$ ps, $I = 150$ mA. (a) CW mode-locking ($L_a = 100$ μm). (b) Unstable mode-locking ($L_a = 120$ μm). (c) Transition from unstable mode-locking to QML ($L_a = 160$ μm). (d) QML ($L_a = 240$ μm).

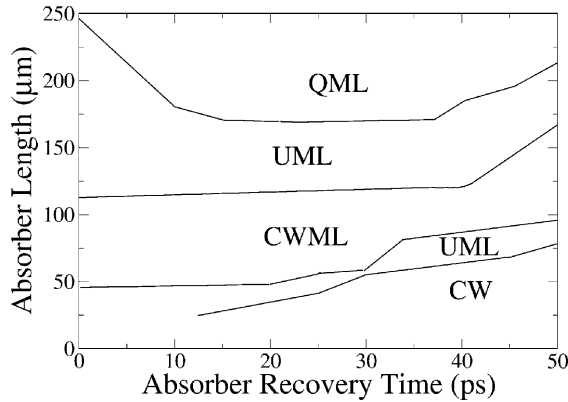


Fig. 5. Phase portrait for 150-mA gain pump current. (CW: Continuous-wave operation, CWML: CW mode-locking, UML: Unstable mode-locked operation, QML: *Q*-switched mode-locking).

pulses being modulated by a *Q*-switched envelope. Typical pulse durations for these forms of mode-locking are 1 to 2 ps.

A sample phase portrait of the different types of behavior obtained from our model is shown in Fig. 5. We vary the length of the absorber section (we keep a constant gain section of 1 mm) and the recombination time within the saturable absorber section for a constant gain current of 150 mA. In practice, the carrier recombination time of the saturable absorber can be changed by varying the reverse bias across it [17]. Here, we consider the range of 5–50 ps for τ_{abs} .

B. *QML*

The mechanism by which QML occurs is quite simple. When the absorber is unsaturated the total loss in the diode cavity exceeds the gain, however by pumping the gain section we increase the carrier density. This continues until the gain, which has increased due to the increase in carriers, exceeds the cavity loss. Noise spikes within the cavity transform into mode-locked pulses in the normal passive mode-locked manner and begin to oscillate in the cavity. This saturates the absorber in a very brief period of time and allows a short and intense pulse to be

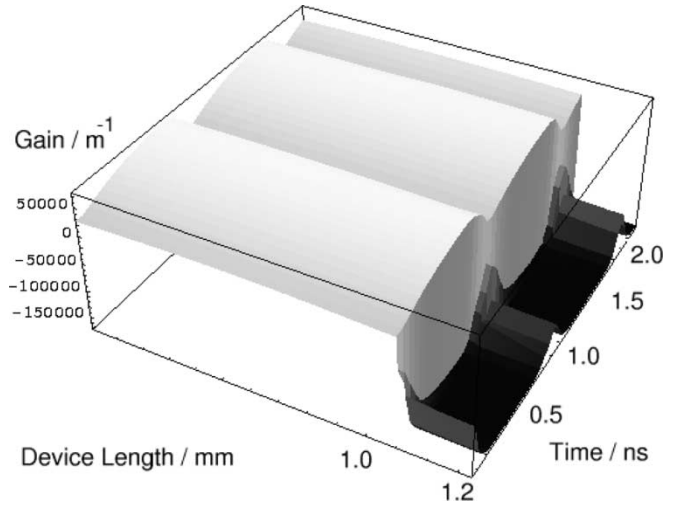


Fig. 6. Gain across the length of the device versus time.

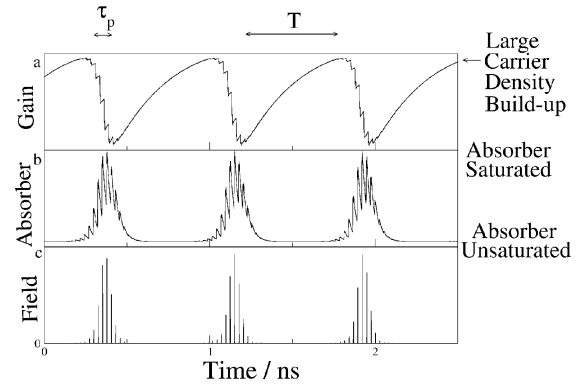


Fig. 7. (a) Gain. (b) Absorber. (c) Output field for device.

emitted. However, this pulse depletes the carrier density, thereby reducing the gain to its original value and preventing pulse generation. Fig. 6 displays the gain across the device versus time as calculated by our model. We can see the gain increase in the absorber section while the saturable absorber maintains a constant absorption. A dip in the gain is then observed with a corresponding peak in the absorption over a time period equal to the pulse duration from the device. Fig. 7 takes a cross-section of the surface generated in Fig. 6 and clearly displays the mechanism previously discussed.

From Fig. 5 we can see how the behavior of the diode can vary quite dramatically over the possible range of parameters. There are regions of the parameter space that allow QML to occur. These are well defined and, therefore, we must be very careful when designing and building our devices to ensure that they will give us a device that will operate in the desired manner. The main requirement for QML is a sufficiently long absorber section which yields a high gain threshold g_{th} for the device. The value of g_{th} can be calculated by finding the equilibrium point between gain and loss in the cavity from

$$\Gamma f_g g_{\text{th}} = \kappa + \frac{1}{2L} \ln \left(\frac{1}{R_1 R_2} \right) + \Gamma f_a \alpha_0 \quad (13)$$

where f_g and f_a are the fraction of the total length of the device L occupied by the gain/absorber respectively and α_0 is the un-

saturated absorption. We have found from both numerical and experimental results that a gain section of 1 mm length and saturable absorber section of 200 μm provides a suitable gain/absorber ratio and also allows for a reasonable frequency tuning range.

C. QML Repetition Frequency Tuning

Fig. 7(a) and (b) displays the behavior of the gain midway through the amplifier and saturable absorber sections respectively for the device output shown in Fig. 7(c). We can clearly see that the repetition frequency of the QML is determined by T . There are several ways by which we can change this T and change the repetition frequency of the device.

The differential gain within the amplifier section determines the slope of the smooth monotonically increasing curve of Fig. 7(a). By varying this value we could change the rate at which the gain increases with carriers. However, in practice we find that we will be working with a certain material which has a specific differential gain and this is not a suitable form of tuning. Similarly we could change the gain saturation terms in the amplifier and/or absorber section. By increasing the gain saturation term it would take a longer period of time for gain-loss equilibrium to be reached. Alternatively we could change the absorber saturation term and set a higher gain to be reached before QML commences. Again though this proves impractical.

We can change the overall cavity loss by placing suitable coatings on the end of the facets of the laser to adjust the end reflectivities. We note that for longer devices this has less of an influence. As can be expected, the length ratio between the gain and the absorber section will be the most important factor in determining the cavity gain-loss dynamics.

Although there are several parameters that play an important role in determining the QML it is only the gain pumping current that provides a convenient way to tune the frequency. The relationship between current and carriers in the gain section is given in (6) and is obviously very strong. A numerically obtained tuning curve is illustrated in Fig. 8. We see that the curve is very similar to Fig. 2, however the device continues to QML for higher currents than experimentally obtained leading to a repetition frequency close to 3.75 GHz. At a current of 170 mA, the modulation depth reduces to less than 100%. This behavior then changes to self-pulsation at 170 mA. This simulation was performed for the same diode laser but with $R_1 = R_2 = 0.95$. We have just considered repetition rates for which we have 100% modulation depth, this limits our maximum achievable repetition frequency. This occurs when $\tau_p \approx T$ and we no longer experience extinction between pulses. These results are similar to those in [18] and [19] where a linear relationship between the repetition rate and current was found for currents well above threshold in the case of just a Q -switched diode laser.

We are also free to change the absorber recovery time as previously explained. This has little effect on the repetition rate as it is the build up in carriers in the gain section that determines T . This was also confirmed experimentally by examining the effect on the RF spectra of changing the saturable absorber reverse bias.

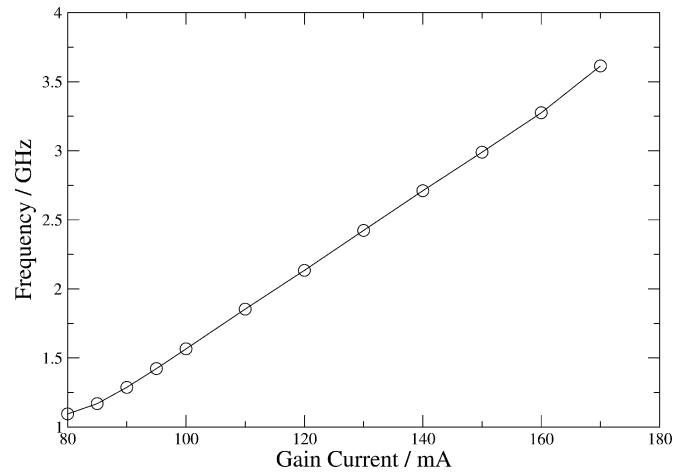


Fig. 8. Numerical tuning curves for up to 3 GHz.

Pulse durations τ_p were found to vary very little with current. The Q -switched pulse envelopes were approximately 100 ps full-width at half-maximum in length. The mode-locked components were approximately 1 ps.

V. CONCLUSION

We have demonstrated QML in a two-section monolithic semiconductor diode laser. We have achieved tuning of the repetition frequency of the QML over a range of 0.4–1.6 GHz by varying the pumping current over the range of 50–100 mA. This yielded an almost linear tuning curve. Detailed numerical modeling was performed on similar diode lasers. It was shown numerically that three distinct forms of mode-locked pulsed behavior possible from these devices depending on the device characteristics. A parameter window in which QML occurred was found to exist for a gain section of 1 mm and an absorber of 0.2 mm. Numerical studies into the gain dynamics of the device were also performed. These illustrated methods by which the tuning range of the device could be extended to much higher frequencies. By simulating our device with end reflectivities of 0.95 we managed to increase the tuning to almost 4 GHz.

ACKNOWLEDGMENT

The authors would like to thank Dr. E. A. Avrutin of the Department of Electronics, University of York, for useful discussions regarding the numerical modeling.

REFERENCES

- [1] E. A. Avrutin, J. H. Marsh, and E. L. Portnoi, "Monolithic and multi-GigaHertz mode-locked semiconductor lasers: Constructions, experiments, models and applications," *Proc. IEE Optoelectron.*, vol. 47, pp. 251–278, Aug. 2000.
- [2] C. Hönninger, R. Paschotta, F. Morier-Genoud, M. Moser, and U. Keller, "Q-switching stability limits of continuous-wave passive mode locking," *J. Opt. Soc. Amer. B*, vol. 16, pp. 46–56, Jan. 1999.
- [3] C. R. Mirasso, G. H. M. van Tartwijk, E. Hernández-García, D. Lenstra, S. Lynch, P. Landais, P. Phelan, J. O'Gorman, M. San Miguel, and W. Elsässer, "Self-pulsating semiconductor lasers: Theory and experiment," *IEEE J. Quantum Electron.*, vol. 35, pp. 764–770, May 1999.
- [4] D. J. Derickson, P. A. Morton, J. E. Bowers, and R. L. Thornton, "Comparison of timing jitter in external and monolithic cavity mode-locked semiconductor lasers," *Appl. Phys. Lett.*, vol. 59, pp. 3372–3374, Dec. 1991.

- [5] Y. K. Chen, M. C. Wu, T. Tanbun-Ek, R. A. Logan, and M. A. Chin, "Subpicosecond monolithic colliding pulse mode-locked multiple quantum well lasers," *Appl. Phys. Lett.*, vol. 58, pp. 1253–1255, Mar. 1991.
- [6] S. Nolte, C. Momma, H. Jacobs, A. Tünnermann, B. N. Chichkov, B. Wellegehausen, and H. Wellin, "Ablation of metals by ultrashort laser pulses," *J. Opt. Soc. Amer. B.*, vol. 14, pp. 2716–2722, Oct. 1997.
- [7] F. H. Loesel, J. P. Fischer, M. H. Götz, C. Horvath, T. Juhasz, F. Noack, N. Suhm, and J. F. Bille, "Non-thermal ablation of neural tissue with femtosecond laser pulses," *Appl. Phys. B, Photophys. Laser Chem.*, vol. 66, pp. 121–128, Jan. 1998.
- [8] P. Tian and W. S. Warren, "Ultrafast measurement of two-photon absorption by loss modulation," *Opt. Lett.*, vol. 27, pp. 1634–1636, Sept. 2002.
- [9] M. Schell, M. Tsuchiya, and T. Kamiya, "Chirp and stability of mode-locked semiconductor lasers," *IEEE J. Quantum. Electron.*, vol. 32, pp. 1180–1190, July 1996.
- [10] J. F. Martins-Filho, E. A. Avrutin, C. N. Ironside, and J. S. Roberts, "Monolithic multiple colliding pulse mode-locked quantum-well lasers: Experiment and theory," *IEEE J. Quantum. Electron.*, vol. 31, pp. 539–551, June 1995.
- [11] S. Bischoff, J. Mørk, T. Franck, S. D. Brorson, M. Hofmann, K. Fröjd, L. Prip, and M. P. Sørensen, "Monolithic colliding pulse mode-locked semiconductor lasers," *Quantum Semiclass. Opt.*, vol. 9, pp. 655–674, Oct. 1997.
- [12] L. M. Zhang and J. E. Carroll, "Dynamic response of colliding-pulse mode-locked quantum-well lasers," *IEEE J. Quantum. Electron.*, vol. 31, pp. 240–243, Feb. 1995.
- [13] M. Ahmed, M. Yamada, and M. Saito, "Numerical modeling of intensity and phase noise in semiconductor lasers," *IEEE J. Quantum. Electron.*, vol. 37, pp. 1600–1610, Dec. 2001.
- [14] D. J. Jones, L. M. Zhang, J. E. Carroll, and D. D. Marcenac, "Dynamics of monolithic passively mode-locked semiconductor lasers," *IEEE J. Quantum. Electron.*, vol. 31, pp. 1051–1058, June 1995.
- [15] S. F. Yu, "Dynamic behavior of vertical cavity surface emitting lasers," *IEEE J. Quantum Electron.*, vol. 32, pp. 1168–1179, July 1996.
- [16] L. M. Zhang, S. F. Yu, M. C. Nowell, D. D. Marcenac, J. E. Carroll, and R. G. S. Plumb, "Dynamic analysis of radiation and side-mode suppression in a second-order DFB laser using time-domain large-signal travelling wave model," *IEEE J. Quantum. Electron.*, vol. 30, pp. 1389–1395, June 1994.
- [17] J. R. Karin, R. J. Helkey, D. J. Derickson, R. Nagarajan, D. S. Allin, J. E. Bowers, and R. L. Thornton, "Ultrafast dynamics in field-enhanced saturable absorbers," *Appl. Phys. Lett.*, vol. 64, pp. 676–678, Feb. 1994.
- [18] M. Kuznetsov, "Pulsations of semiconductor lasers with a proton bombarded segment: Well-developed pulsations," *IEEE J. Quantum. Electron.*, vol. QE-21, pp. 587–592, June 1985.
- [19] R. W. Dixon and W. B. Joyce, "A possible model for sustained oscillations (pulsations) in (AlGa)As double-heterostructure lasers," *IEEE J. Quantum. Electron.*, vol. QE-15, pp. 470–474, June 1979.



Michael B. Flynn (S'02) received the B.Sc. degree (with first class joint honors) in applied mathematics and physics from University College Cork, Ireland, in 2001. He is currently pursuing the Ph.D. degree in the modeling of various semiconductor and photonic crystal devices at the University of St. Andrews, North Haugh, Fife, U.K. His other research interests include nonlinear optics and ultrashort pulse generation and propagation.



Liam O'Faolain received the B.Sc. degree (with honors) in physics from the National University of Ireland, Cork, Ireland, in 2001. He is currently pursuing the Ph.D. degree at the University of St. Andrews, North Haugh, Fife, U.K., on mode-locked semiconductor lasers diodes.



Thomas F. Krauss received the Ph.D. degree from Glasgow University, U.K., on the topic of monolithic semiconductor ring lasers, where he was the first to demonstrate continuous-wave operation as well as OEIC functionality.

He has been involved in optoelectronics research for the past 15 years since working at IBM, Yorktown Heights, N.Y. (1987–1988). As a Royal Society Research Fellow, he initiated the field of semiconductor photonic crystals in the U.K. (1993) and has since established a reputation worldwide, as evidenced by the large number of invited talks he presents at international level (14 such presentations in 2002 alone). In 1997, he spent a year at Caltech, Pasadena, CA, to work on efficient photonic crystal-based light emitters. In 2000, he accepted a Personal Chair in Optoelectronics at the School of Physics and Astronomy, University of St. Andrews, North Haugh, Fife, U.K., and established a photonic crystal research group (currently ten members) and semiconductor microfabrication laboratory. He is grant holder of several U.K. research projects and was coordinator of the FP5-IST research project "Photonic Integrated Circuits using Photonic Crystals (PICCO)" involving seven academic and industrial partners from Belgium, Denmark, Italy, and the U.K.

Dr. Krauss was elected a Fellow of the Institute of Physics in 2001 and the Royal Society of Edinburgh in 2002.